REPORT DOCUMENTATION PAGE

AFRL-SR-BL-TR-01-

0367

Public reporting burden for this collection of information is estimated to average 1 hour per response, including the gathering and maintaining the data needed, and completing and reviewing the collection of information. Send cor collection of information, including suggestions for reducing this burden, to Washington Headquarters Services, Di Davis Highway, Suite 1204, Arlington, VA 22202-4302, and to the Office of Management and Budget, Paperwork .

1. AGENCY USE ONLY *(Leave blank)*	2. REPORT DATE	3. REPORT TYPE AND DATES COVERED
		Final Technical Report 01 Apr 00 - 31 Mar 01

4. TITLE AND SUBTITLE	5. FUNDING NUMBERS
Upgrade of the Computing and Visualization System for DNS/LES Research	F49620-00-1-0220

6. AUTHOR(S)
Dr. Chaoqun Liu

7. PERFORMING ORGANIZATION NAME(S) AND ADDRESS(ES)	8. PERFORMING ORGANIZATION REPORT NUMBER
College of Engineering & Science Louisana Tech University P.O. Box 10348 Ruston, LA 71272-0001	

9. SPONSORING/MONITORING AGENCY NAME(S) AND ADDRESS(ES)	10. SPONSORING/MONITORING AGENCY REPORT NUMBER
AFOSR/NM 801 N. Randolph St, Rm 732 Arlington, VA 22203-1977	F49620-00-1-0220

11. SUPPLEMENTARY NOTES

12a. DISTRIBUTION AVAILABILITY STATEMENT	12b. DISTRIBUTION CODE
Approved for public release; distribution unlimited.	AIR FORCE OFFICE OF SCIENTIFIC RESEARCH (AFOSR) NOTICE OF TRANSMITTAL DTIC THIS TECHNICAL REPORT HAS BEEN REVIEWED AND IS APPROVED FOR PUBLIC RELEASE LAW AFR 190-12. DISTRIBUTION IS UNLIMITED.

13. ABSTRACT *(Maximum 200 words)*

The Defense University Research Instrument Prograln (DURIP) grant, Upgrade of the Computing and Visualization System for DNS/LES Research, Grant No. F49620-00-1-0220 for $400,000 hms been mainly spent for upgrading the existing SGI Origin 2000 from 16 CPU to 32 CPU with additional 6 GB memory and over 200 GB hard disk. A 8 cpu SGI 1200L clustered system and a number of SGI and Dell Workstations and PCs have also been purchased by this fund. These purchases and upgrading have greatly strengthen Louisiana Tech University in conducting Defense related research and education. Dr. Liu's DNS/LES group has got permission to access all theses systems to conduct their state-of-the art DNS/LES research which has been supported by AFOSR for a number of years. They have used that system to conduct DNS/LES computation for 3-D airfoils and plan to work for simplified aircrafts.

20010625 154

14. SUBJECT TERMS			15. NUMBER OF PAGES
			22
			16. PRICE CODE

17. SECURITY CLASSIFICATION OF REPORT	18. SECURITY CLASSIFICATION OF THIS PAGE	19. SECURITY CLASSIFICATION OF ABSTRACT	20. LIMITATION OF ABSTRACT
UNCLASSIFIED	UNCLASSIFIED	UNCLASSIFIED	UL

Standard Form 298 (Rev. 2-89) (EG)
Prescribed by ANSI Std. 239.18
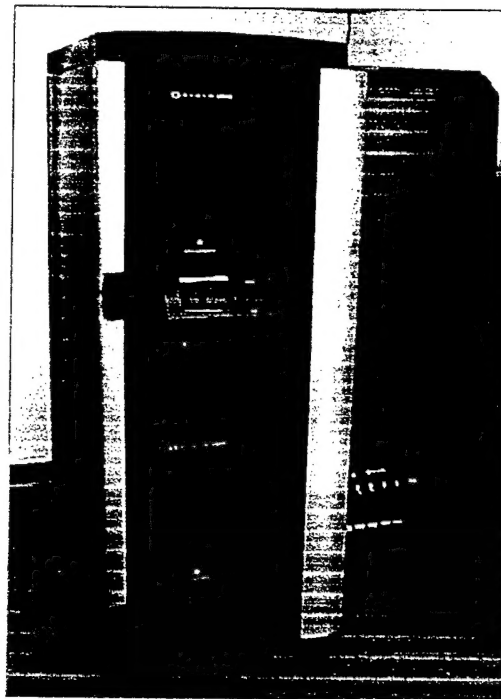Designed using Perform Pro, WHS/DIOR, Oct 94

FINAL REPORT

Upgrade of the Computing and Visualization System for DNS/LES research

F49620-00-1-0220

4/1/00-3/30/01

Program Manager:

Dr. Robert Herklotz
AFOSR, Room 732
801 North Randolph Street
Arlington, VA 22203-1977
Phone: (703) 696-6565
Fax: (703) 696-8450

Principal Investigator:

Dr. Chaoqun Liu, Professor
College of Engineering & Science
Louisiana Tech University
P.O.Box 10348
Ruston, LA 71272-0001
Phone: (318) 257-4647
E-mail: cliu@engr.LaTech.edu

May 1, 2001

Upgrade of the Computing and Visualization System for DNS/LES Research
(Final Report)

From
Dr. Chaoqun Liu, Professor
College of Engineering and Science
Campus Box 10, P.O. Box 10348
CTH 128
Louisiana Tech University
Ruston, LA 71272-0001
Tel : (318) 257-4647
Fax : (318) 257-3290

To
Dr. Robert Herklotz
Air Force Office of Scientific Research
Room 732
801 North Randolph Street
Arlington, VA 22203-1977 Phone : (703) 696-6565
Fax : (703) 696-8450

May 1, 2001

Table of Contents

ABSTRACT

The Defense University Research Instrument Program (DURIP) grant, Upgrade of the Computing and Visualization System for DNS/LES Research, Grant No. F49620-00-1-0220 for $400,000 has been mainly spent for upgrading the existing SGI Origin 2000 from 16 CPU to 32 CPU with additional 6 GB memory and over 200 GB hard disk. A 8 cpu SGI 1200L clustered system and a number of SGI and Dell Workstations and PCs have also been purchased by this fund. These purchases and upgrading have greatly strengthen Louisiana Tech University in conducting Defense related research and education. Dr. Liu's DNS/LES group has got permission to access all theses systems to conduct their state-of-the art DNS/LES research which has been supported by AFOSR for a number of years. They have used that system to conduct DNS/LES computation for 3-D airfoils and plan to work for simplified aircrafts.

1 List of Purchases

32-4226-56131
UPGRADE OF COMPUTING & VISUALIZATION SYSTEM

PR #	Vendor	Item	Cost
54 4537	SGI	Upgrade SGI Origin 2000 SGI Octane 2 V6 Graphics Workstation 8 SGI 1200L Clustered Dual System	338,979.55
60 2801	Rexel Summers	HBL2620 Hub	24.23
60 2847	Murco	Cutler Hammer Disconnect Switch	39.89
60 2809	Dell Marketing	4 PIII Desktop Workstations	16,820.24
59 4980	Base Distributors	Tripplite Smart Datacenter 5000 HR 5KVA extended runtime LAN UPS system	3,199.00
61 7041	Reimburse Mel Corley	VMWare Software for Windows NT & 2000	99.00
60 1500	Reimburse Carey Cox	VMWare Software for Windows NT & 2000	99.00
60 4583	Reimburse Mel Corley	VIA Video Conferencing Software	314.87
61 7073	Dell Marketing	4 Back-up Pro	716.00
60 1493	Portland Group Inc.	Linux Server Software	1,599.00
61 6804	Dell Marketing	Inspiron 8000, Pentium III, Notebook Computer	3,358.95
61 2625	SGI	3 18.2GB Hard Drives; 1 AMP Power Distribution Unit	1,642.74
61 2627	Dell Marketing	3Com SuperStack 3 Baseline 10/100 Switch 24 port; 8 LAN Utp Cat 5 Patch Cables; OmniView Pro 16 Port KVM Switch w/on-screen display	1,139.55
61 2623	Dell Marketing	Poweredge 1550	12,246.56
61 2622	Dell Marketing	PowerVault 120T, DLT1, Desktop 5 Black Watch DLT IV	4,123.90 365.00
61 2674	Dell Marketing	2 1.50GHz, P4, DellPrecision 330, Mini Towers	9,890.52
61 6801	PC Connection	Ceiling Mount for PowerLite Projector; Epson Powerlite ELP-5350	4,686.00
61 2697	XYZ Scientific	TrueGrid Software	500.00
61 2675	Dell Marketing	CD-RW Drive	156.00
		TOTAL	400,000.00

2 Rationale of the purchase

2.1 Upgrade of the SGI Origin 2000 Computer

Our research project, Parallel Multigrid DNS/LES Methods for Time-Dependent Compressible Turbulent Flow Around 3-D Airfoils (AFOSR Grant F49620-99-1-0042, F49620-01-1-0065), is required to solve one of the most difficult fluid dynamics problems which demands utilization of thousands of supercomputer hours. To avoid waiting for days or even weeks on a busy CRAY user's queue and many hours for huge data transfer from CRAY to our local computer for each computational job, we purchased an SGI Origin 2000 with 16 CPUs and 4 GB memory by a AFOSR grant and Louisiana Tech matching fund in July 1998 at a total cost of $300,000. This SGI parallel computer has greatly increased our computational capability and dramatically accelerated our research. However, as the research steps up to the stage of DNS/LES for 3-D airfoils and wing-fuselage combination, we have to use much more grid points which requires huge memory and CPU time. By this DURIP grant, we have upgraded our system by increasing additional 6 GB memory and 16 processors. We also increased additional 227 GB hard disk for our huge DNS/LES data base and visualization. This upgrade enable us to have 10 GB memory, 300 GB hard disk and 32 processors on the SGI Origin 2000 system which will be able to handle 3-D time-dependent problems with more than 30 million grid points. It is critical to the success of our AFOSR research project.

SGI Origin 2000 is an advanced shared memory machine with CRAY linkage technology which is scalable for large number of processors. SGI also has a so-called VARSITY program which can provide half-million dollar software package including Fortran 90, C++, and MPI to users for an annual cost of three thousand dollars. In addition, SGI has a nice reputation for its graphic technology.

We also purchased SGI Cluster with 8 CPUs and a number of SGI and Dell Workstations and PCs to support the system and provide students and researchers to conduct defense related research and education.

2.2 Impact on the DNS/LES Research Project

The Center for Numerical Simulation and Modeling (CNSM) which is previously called Numerical Simulation Group led by Dr. Chaoqun Liu, has a long history working on DNS/LES for complex turbulent flow. Since it moved to Louisiana Tech University in 1996, CNSM has formed a DNS/LES team which consists of faculty, post doctors and PhD students with expertise in grid generation, numerical scheme, flow solver, turbulence modeling, and visualization under AFOSR support. The University has provided $120,000 for purchase of equipment and around 4000 square feet space with air condition and technical support to house the research group and equipment. Now, CNSM has become one of the major DNS/LES research groups around the nation and a major computational research center in the University. Dr. Liu's group has moved to UT-Arlington, but got permission from La Tech to access all these computing and visualization systems for their AFOSR research project.

With this grant we are able to have 32 processors, 10 GB memory, and 300 GB hard disk drive which has doubled our capability to conduct DNS/LES for more complex geometry and higher Reynolds number. The quality of research and education will be significantly improved.

2.3 Impact on Research Related Education

The interdisciplinary PhD curriculum, the Mathematics, and the Computer Science MS program at Louisiana Tech University include several courses related to computation. These courses are designed to meet the dramatically growing demand for expertise in parallel computation by the industrial market. With this upgrading, CNSM now can provide these students more opportunities to practice the parallel computing techniques. High-performance C++, C, and Fortran compilers have already been installed, as well as the Message Passing Interface (MPI) package. The virtual reality system which was purchased by a Louisiana State grant and supported by the SGI system can also be used as a means to assistant these students to improve their ability to conduct visualization and data analysis. The upgrade of this SGI computer has attracted more graduate students to work for future DoD-sponsored programs and significantly enhance the capability of Louisiana Tech University to conduct DoD research-related education.

This project also gives a significant impact on faculty development. In general, the quality of faculty determines the quality of research. This will significantly improve the level of computational facilities available to the faculty, thereby permitting CNSM to attract and retain better faculty and post doctors. Existing faculty can achieve computational results at levels not otherwise possible, thereby enhancing career advancement and improving the quality of research and education.

2.4 Impact on the DNS/LES Community

CNSM has hosted the First AFOSR International Conference on DNS/LES in 1997 which attracted 93 participants from 16 countries around the world. The AICDL conference is a major conference in the world which is focused on DNS/LES. CNSM will organize the Third AFOSR International Conference on DNS/LES in August 2001, which means CNSM will organize this important DNS/LES conference twice within four years. CNSM has been recognized as a notable DNS/LES research center by the world DNS/LES community.

The success of the AFOSR project will clearly show the global DNS/LES community that US is leading the world in DNS/LES research and pushing DNS/LES for practical engineering applications.

The DURIP grant has played an important role to the success of our AFOSR DNS/LES research project, the DoD project related education, and the US reputation of leading the world in basic research on turbulence.

3 Current AFOSR Research Project

We currently conduct AFOSR research project, Numerical Simulation of Flow Instability around a Delta Wing.

Recent developments in aerospace technology have revived the interest to the study of flow separations around an aircraft maneuvering dynamic operations. Understanding of the complex separated vortical flow is crucial to the aerodynamic design of modern aircraft. Vortical structures, which develop over the leading-edge extension, slender fore-body, and main wing, may have severe

effect on the aerodynamic characteristics and performance of modern fighter aircraft.

A flat-plate delta wing with sharp leading-edge provides a simple configuration to investigate the development of the vortical structures. Both experimental and computational results have shown that the flow over the suction side of a delta wing at a fixed angle of attack is dominated by a pair of counter-rotating vortices, i.e. the leading-edge primary vortices. These vortices are formed as a result of the rolling-up of the vortex sheet shedding from the leading-edge. The flow induced by the leading-edge vortices separates near the wing surface and forms a pair of oppositely rotating secondary vortices. The size and strength of the leading-edge vortices increase with the angle of incidence, resulting in a substantial nonlinear lift increment. But the maximum lift of a delta wing is limited by a phenomenon known as vortex breakdown(Visser & Nelson 1993).

In the experimental study using dye visualization carried out by Gad-el-Hak and Balckwelder (1985), small-scale vortices were observed shedding from the leading-edge and feeding into the rolling-up process associated with the large-scale leading-edge vortices. In their study, the small-scale vortices were paired, and were believed as the origination of the classical leading-edge vortices. Payne et al. (1988) used smoke flow visualization and laser sheet technique to study the vortical flow field above the delta wing at high angles of attack. Two types of vortex breakdown were testified, i.e. the bubble mode and the spiral mode. In the same experiment, static small-scale vortical-like structures were found in the shear layer of a delta wing with a 85° sweep angle and a 40° angle of attack. The growth of these structures was found to be similar to the evolution of the classic Kelvin-Helmholtz instability. In this experiment, the pairing of the small-scale vortices was not observed. The recent experimental work of Rieley & Lowson (1998) revealed, using flow visualization and hot-wire measurement, the existence of static small vortical structures in the free shear layer shedding from the sharp leading-edge of a delta wing. A local three-dimensional Kelvin-Helmholtz-type instability was suggested by the authors for the formation of these vortical structures in the free shear layer. Similar vortical structures were also observed in the investigations of Cipolla & Rockwell (1998), where small-scale concentrations of vorticity form near the leading-edge of a rolling delta wing. These vortices appear to evolve in a coupled fashion, which has been considered as the wake-like instability.

Numerical simulations of vortex breakdown above a stationary sharp edged delta wing over a range of angles of attack were carried out by Modiano & Murman (1994). Their computation was based on an Euler solver with adaptive mesh system. The spiral form of vortex breakdown was observed without the emergence of the small-scale vortical structures inside the shear layer. In the numerical investigation by Argwal et al. (1992), the well-known Euler/Navier-Stokes code CFL3D was used to simulate the leading-edge vortex breakdown of a low-speed flow on a flat-plate delta wing with sharp leading-edges. Although the vortex breakdown positions obtained from the computation were reported in good agreement with experimental data, the small-scale vortices were not observed, which could be attributed to the lack of numerical resolution/accuracy. A numerical investigation of the unsteady vortex structure over a 76° sweep wing at 20.5° angle of attack was carried out by Gordnier & Visbal (1994). Their numerical calculation indicated that the small-scale vortical structures emanated from the leading-edge was brought on by the Kelvin-Helmholtz-type instability. Pairing of the small vortices was not observed in the computational results.

The intention of present work is to study the mechanism of vortex breakdown above a slender flat-plate delta wing with sharp leading-edges at a fixed angle of attack. Direct numerical simulation is employed to give a detailed description of flow instability and vortex shedding near the leading-

edge of the delta wing.

3.1 Governing Equations

The three-dimensional compressible Navier-Stokes equations in generalized curvilinear coordinates (ξ, η, ζ) are written in conservative forms:

$$\frac{1}{J}\frac{\partial Q}{\partial t} + \frac{\partial(E - E_v)}{\partial \xi} + \frac{\partial(F - F_v)}{\partial \eta} + \frac{\partial(G - G_v)}{\partial \zeta} = 0 \tag{1}$$

The flux vectors for compressible flow are

$$Q = \begin{pmatrix} \rho \\ \rho u \\ \rho v \\ \rho w \\ e \end{pmatrix}$$

$$E = \frac{1}{J}\begin{pmatrix} \rho U \\ \rho U u + p\xi_x \\ \rho U v + p\xi_y \\ \rho U w + p\xi_z \\ U(e + p) \end{pmatrix}$$

$$F = \frac{1}{J}\begin{pmatrix} \rho V \\ \rho V u + p\eta_x \\ \rho V v + p\eta_y \\ \rho V w + p\eta_z \\ V(e + p) \end{pmatrix}$$

$$G = \frac{1}{J}\begin{pmatrix} \rho W \\ \rho W u + p\zeta_x \\ \rho W v + p\zeta_y \\ \rho W w + p\zeta_z \\ W(e + p) \end{pmatrix}$$

$$E_v = \frac{1}{J}\begin{pmatrix} 0 \\ \tau_{xx}\xi_x + \tau_{yx}\xi_y + \tau_{zx}\xi_z \\ \tau_{xy}\xi_x + \tau_{yy}\xi_y + \tau_{zy}\xi_z \\ \tau_{xz}\xi_x + \tau_{yz}\xi_y + \tau_{zz}\xi_z \\ q_x\xi_x + q_y\xi_y + q_z\xi_z \end{pmatrix}$$

$$F_v = \frac{1}{J}\begin{pmatrix} 0 \\ \tau_{xx}\eta_x + \tau_{yx}\eta_y + \tau_{zx}\eta_z \\ \tau_{xy}\eta_x + \tau_{yy}\eta_y + \tau_{zy}\eta_z \\ \tau_{xz}\eta_x + \tau_{yz}\eta_y + \tau_{zz}\eta_z \\ q_x\eta_x + q_y\eta_y + q_z\eta_z \end{pmatrix}$$

8

$$G_v = \frac{1}{J} \begin{pmatrix} 0 \\ \tau_{xx}\zeta_x + \tau_{yx}\zeta_y + \tau_{zx}\zeta_z \\ \tau_{xy}\zeta_x + \tau_{yy}\zeta_y + \tau_{zy}\zeta_z \\ \tau_{xz}\zeta_x + \tau_{yz}\zeta_y + \tau_{zz}\zeta_z \\ q_x\zeta_x + q_y\zeta_y + q_z\zeta_z \end{pmatrix}$$

where J is Jacobian of the coordinate transformation, and $\xi_x, \xi_y, \xi_z, \eta_x, \eta_y, \eta_z, \zeta_x, \zeta_y, \zeta_z$ are coordinate transformation metrics. τ_{kl}'s and q_k's are the viscous stress and the heat flux, respectively.

In Eq. (1), second order Euler Backward scheme is used for time derivatives, and the fully implicit form of the discretized equations is:

$$\frac{3Q^{n+1} - 4Q^n + Q^{n-1}}{2J\Delta t} + \frac{\partial(E^{n+1} - E_v^{n+1})}{\partial \xi}$$
$$+ \frac{\partial(F^{n+1} - F_v^{n+1})}{\partial \eta} + \frac{\partial(G^{n+1} - G_v^{n+1})}{\partial \zeta} = 0$$

(2)

Q^{n+1} is estimated iteratively as:

$$Q^{n+1} = Q^p + \delta Q^p \tag{3}$$

where,

$$\delta Q^p = Q^{p+1} - Q^p \tag{4}$$

At step $p = 0$, $Q^p = Q^n$; as δQ^p is driven to zero, Q^p approaches Q^{n+1}. Flux vectors are linearized as follows:

$$E^{n+1} \approx E^p + A^p \delta Q^p$$
$$F^{n+1} \approx F^p + B^p \delta Q^p$$
$$G^{n+1} \approx G^p + C^p \delta Q^p$$

(5)

So that Eq. (2) can be written as:

$$[\frac{3}{2}I + \Delta t J(D_\xi A + D_\eta B + D_\zeta C)]\delta Q^p = R \tag{6}$$

where R is the residual:

$$R = -(\frac{3}{2}Q^p - 2Q^n + \frac{1}{2}Q^{n-1}) - \Delta t J[(D_\xi(E - E_v)$$
$$+ D_\eta(F - F_v) + D_\zeta(G - G_v)]^p$$

D_ξ, D_η, D_ζ represent partial differential operators, and A, B, C are the Jacobian matrices of flux vectors:

$$A = \frac{\partial E}{\partial Q}, \qquad B = \frac{\partial F}{\partial Q}, \qquad C = \frac{\partial G}{\partial Q} \tag{7}$$

The right hand side of Eq. (6) is discretized using fourth-order compact scheme (Lele, 1992) for spatial derivatives, and the left hand side of the equation is discretized following LU-SGS method (Yoon & Kwak, 1992). In this method, the Jacobian matrices of flux vectors are split as:

$$A = A^+ + A^-, \quad B = B^+ + B^-, \quad C = C^+ + C^-$$

9

where,

$$A^{\pm} = \frac{1}{2}[A \pm r_A I]$$

$$B^{\pm} = \frac{1}{2}[B \pm r_B I] \qquad (8)$$

$$C^{\pm} = \frac{1}{2}[C \pm r_C I]$$

and,

$$r_A = \kappa max[|\lambda(A)|] + \tilde{\nu}$$

$$r_B = \kappa max[|\lambda(B)|] + \tilde{\nu}$$

$$r_C = \kappa max[|\lambda(C)|] + \tilde{\nu}$$

where $\lambda(A), \lambda(B), \lambda(C)$ are eigenvalues of A, B, C respectively, κ is a constant greater than 1. $\tilde{\nu}$ is taken into account for the effects of viscous terms, and the following expression is used:

$$\tilde{\nu} = max[\frac{\mu}{(\gamma - 1)M_r^2 R_e P_r}, \frac{4}{3}\frac{\mu}{R_e}]$$

The first-order upwind finite difference scheme is used for the split flux terms in the left hand side of Eq. (6). This does not effect the accuracy of the scheme. As the left hand side is driven to zero, the discretization error will also be driven to zero. The finite difference representation of Eq. (6) can be written as:

$$[\frac{3}{2}I + \Delta t J(r_A + r_B + r_C)I]\delta Q_{i,j,k}^p = R_{i,j,k}^p$$

$$-\Delta t J \quad [\quad A^-\delta Q_{i+1,j,k}^p - A^+\delta Q_{i-1,j,k}^p$$

$$+ \quad B^-\delta Q_{i,j+1,k}^p - B^+\delta Q_{i,j-1,k}^p$$

$$+ \quad C^-\delta Q_{i,j,k+1}^p - C^+\delta Q_{i,j,k-1}^p \quad] \qquad (9)$$

In LU-SGS scheme, Eq. (9) is solved by three steps. First initialize δQ^0 using

$$\delta Q_{i,j,k}^0 = [\frac{3}{2}I + \Delta t J(r_A + r_B + r_C)I]^{-1}R_{i,j,k}^p$$

In the second step, the following relation is used:

$$\delta Q_{i,j,k}^* = \delta Q_{i,j,k}^0 + [\frac{3}{2}I + \Delta t J(r_A + r_B + r_C)I]^{-1}$$

$$\times [\Delta t J(A^+\delta Q_{i-1,j,k}^* + B^+\delta Q_{i,j-1,k}^* + C^+\delta Q_{i,j,k-1}^*)]$$

For the last step, δQ^p is obtained by

$$\delta Q_{i,j,k}^p = \delta Q_{i,j,k}^* - [\frac{3}{2}I + \Delta t J(r_A + r_B + r_C)]^{-1}$$

$$\times [\Delta t J(A^-\delta Q_{i+1,j,k}^p + B^-\delta Q_{i,j+1,k}^p + C^-\delta Q_{i,j,k+1}^p)]$$

The sweeping is performed along the planes of $i+j+k = const$, i.e. in the second step, sweeping is from the low-left corner of the grid to the high-right corner, and then vice versa in the third step.

In order to depress numerical oscillation caused by central difference scheme, spatial filtering is used instead of artificial dissipation. Implicit sixth-order compact scheme for space filtering (Lele, 1992) is applied for primitive variables u, v, w, ρ, p after each time step.

For subsonic flow, u, v, w, T are prescribed at the inflow boundary, ρ is obtained by solving modified N-S equation based on the characteristic analysis. On the far field and out flow boundary, non-reflecting boundary conditions are applied. Adiabatic, non-slipping conditions are used for the wall boundary. All equations of boundary conditions are solved implicitly with internal points. Specific details of boundary treatment can be found in Jiang et al (1999).

3.2 Computational Details

Direct numerical simulation has been implemented to investigate the compressible flow separation around a slender delta wing. The geometry of the delta wing, taken from the experimental work of Rieley & Lowson (1998), is shown in Figure 1. The sweep angle denoted by Λ is 80° and the leading-edge angle denoted by σ is 30°. The chord length is taken as the characteristic length L, such that the non-dimensional chord length is $c = 1.0L$. The non-dimensional thickness of the delta wing is $h = 0.024L$. The freestream velocity U_∞ is the characteristic velocity.
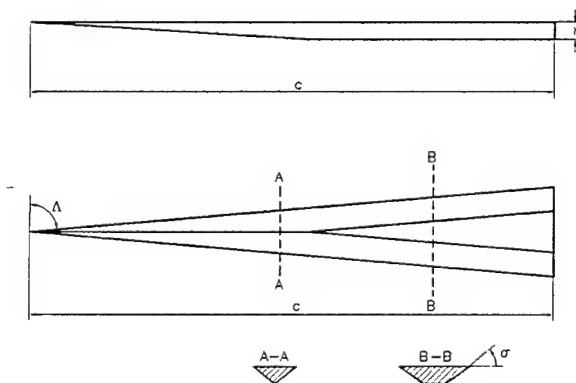

Figure 1: Schematic of the delta wing

An H-C type mesh system for a half-plane model of the delta wing is used based on the assumption that the flow is symmetrical to the the half-plane. The mesh is H-type in the meridian section and C-type in the cross section. An elliptic grid generation method, first proposed by Spekreijse (1995), is used to generate the three-dimensional grids. This method is based on a composite mapping, which is consisted of a nonlinear transfinite algebraic transformation and an elliptic transformation. The grids are orthogonal on the delta wing surface. The sharp leading-edge is approximated by a round edge with a small radius of $1.0 \times 10^{-3}L$, while in the experiment of Rieley & Lowson (1998), the average thickness of the leading-edge was 0.12 mm, which was approximately $2.55 \times 10^{-4}L$. Computations are carried out on two grid systems, i.e. the low resolution mesh with $140 \times 70 \times 70$ grid nodes and the high resolution mesh with $180 \times 150 \times 70$ grid nodes, where the sequence of numbers is corresponding to the axial, the spanwise and the wall-normal direction, respectively. An example of the three-dimensional grid is displayed in Figure 2.

The parallel version of the DNS code based on the Message Passing Interface (MPI) has been
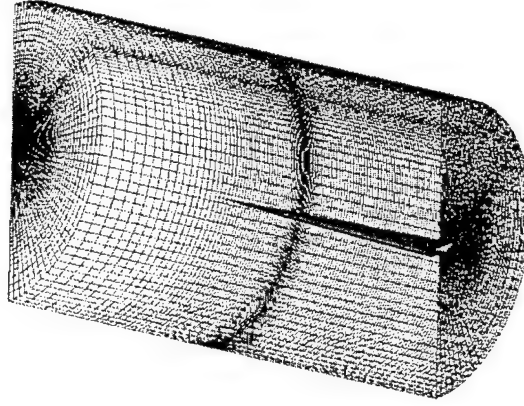
Figure 2: H-C type grid around a 85° sweep delta wing

developed to accelerate the computation. Although massive data exchanges are required for computing the derivatives with the compact finite difference scheme, the speedup is still substantial. On a SGI Origin 2000 computer, the performance of the MPI code is superior to the serial code, which is compiled using the automatic parallelization option provided by Fortran 90 compiler. The comparison are displayed in Figure 3, where the speedup parameter $S(n,p)$ is defined as the ratio of the runtime of a serial solution to a problem to the parallel runtime. Linear speedup has been achieved for MPI code running on 4, 6, and 15 processors. The final parallel computation for the higher Reynolds number case with a mesh of $180 \times 150 \times 70$ is conducted using 10 processors on a SGI Origin 2000 computer.
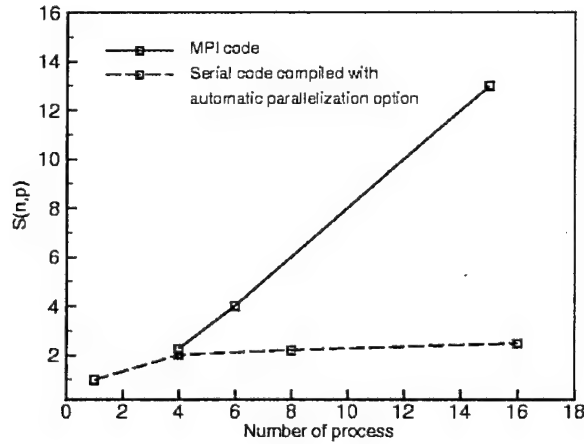

Figure 3: Speedup $S(n,p)$ of the MPI code compared with the serial code complied with automatic parallelization option

3.3   Results and Discussions

3.3.1   Low Reynolds number case

All results presented here are obtained from direct numerical simulation of flow around a 85° sweep delta wing with a flat-plate suction surface, which has been introduced in Section 3. The angle of attack is fixed at 12.5°. The free-stream Mach number is $Ma = 0.1$. For the lower resolution simulation, the Reynolds number based on the chord length and the free-stream velocity is $Re_c = 5 \times 10^4$. No initial and boundary disturbance are imposed in the simulation.

The contours of the axial vorticity on selected cross sections are displayed in Figure 4. It is quite clear that a pair of counter-rotating vortices, so called the leading-edge primary vortices, appears over the suction side of the delta wing. These vortices form as a result of flow separation and the rolling-up of the vortex sheet shedding from the leading-edge. The primary vortices are steady and stable in this low Reynolds number case. The primary vortices are composed of a pair of counter-rotating oblique vortex tubes starting from the apex of delta wing, from a three-dimensional point of view. Beneath the primary vortices, near the upper surface of the delta wing, the secondary vortices, which have an opposite rotating direction to the primary vortices, are formed as a result of the spanwise outflow induced by the primary vortex. Figure 5 shows the three-dimensional instantaneous streamlines starting from vicinity of the leading-edge. The streamlines also reveals the existence of the cone-shaped primary vortices. The computational results are in good agreement with the experimental results of Riley & Lowson (1998). During the computation for the high Reynolds number case, the flow becomes unsteady and small-scale vortical structures keep shedding from the leading-edge. In the experiment of Riley & Lowson (1998), flow instability was observed when the Reynolds number was raised above $Re_c = 100,000$. In order to study the flow instability near the leading edge, the numerical simulation with a higher resolution and higer Reynolds number has been implemented, and the results are discussed in next section.
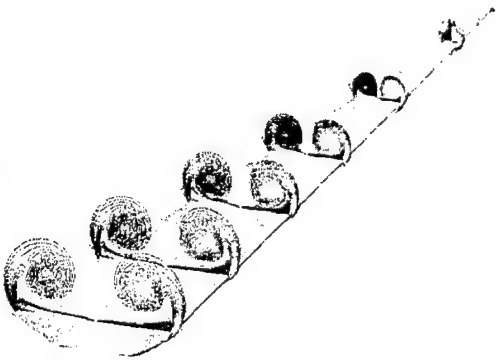

Figure 4: Contours of the axial vorticity on selected cross sections, angle of attack $\alpha = 12.5°$, $Re = 5 \times 10^4$, $Ma = 0.1$
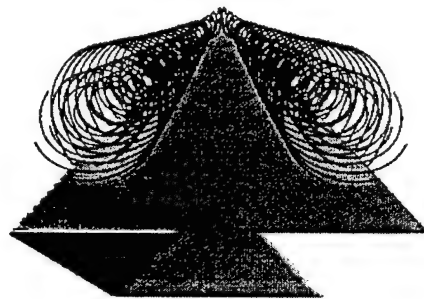
Figure 5: Three-dimensional streamline above the suction surface of a 85° sweep delta wing at an angle of attack $\alpha = 12.5°$, $Re = 5 \times 10^4$, $Ma = 0.1$

3.3.2 High Reynolds number case

At higher Reynolds number, i.e. $Re_c = 1.96 \times 10^5$, which is the same as the one chosen by Riley & Lowson (1998) in their experimental study, where the flow instability occurs near the leading edge of the delta wing. In order to capture the small vortical structures observed in the experiment, the numerical simulation is accomplished on a mesh with a higher resolution of $180 \times 150 \times 70$. During the simulation, flow instability and periodic shedding of small vortical structures are observed. Since there is no disturbance imposed as the initial or boundary condition for the computation, the unstable behavior presented by the flow in the computational results are rather intrinsic.

The distributions of the instantaneous axial vorticity on various cross sections are shown in Figure 6. Compared with the low Reynolds number results of Figure 4, the flow is still dominated by a pair of primary vortices. But instability appears at the leading-edge of delta wing, where vortex shedding is observed. On the suction surface near the leading-edge, the secondary vortices are still visible in this figure.
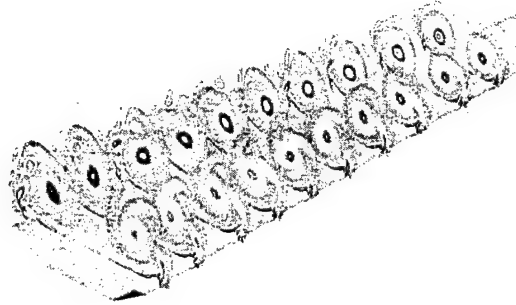

Figure 6: The instantaneous distributions of the axial vorticity on various cross sections. Angle of attack $\alpha = 12.5°$, $Re = 1.96 \times 10^5$, $Ma = 0.1$

In Figure 7 the contours of axial vorticity at different time on a cross section at $x = 0.87L$ are displayed through (a) to (h), each frame is corresponding to a snapshot of a two-dimensional flow field at a certain time. Flow instability is quite obvious in these figures. The primary vortex deforms compared to the low Reynolds number case. The flow pattern inside the primary vortex resembles that of the spiral instability mode, which presented occasionally in the experiment of Rieley & Lowson(1998). Two strong shear layers are visible through the concentration of axial vorticity contours. The first one is the leading-edge shear layer whose axial vorticity is positive (shown in light color in Figure 7), which wraps the leading-edge corner from below and feeds into the primary vortex. The other one lies between the primary vortex and the upper surface of the delta wing and has a negative axial vorticity (shown in dark color in Figure 7), which is associated with the secondary vortex. Therefore, the shear layer below the primary vortex is also called the secondary shear layer. As it will be discussed later, both the leading-edge shear layer and the secondary shear layers are related to the instability and vortex shedding procedure near the leading-edge.

Among the small-scale vortical structures shedding from the leading-edge, there are two types of vortices, distinguished by the direction of rotation or by the sign of axial vorticity. Those vortices whose rotating direction is the same as the primary vortex are named as the A-family vortices,

14

which are corresponding to a positive axial vorticity component. The vortices rotating in the opposite direction as the primary vortex are called the B-family vortices and have a negative axial vorticity component. The A-family vortices are much stronger than the B-family vortices, which can be recognized from the contours of the axial vorticity in Figure 7.

In Figure 7(a), a bulge is observed on the leading-edge shear layer. The bulge grows in size as it moves away from the leading edge, as shown in Figure 7(b), (c), and (d). This process is corresponding to the generation and shedding of the A-family vortex. Because the B-family vortices are very weak, the shedding process of B-family vortices is not clear in Figure 7. A more detailed study reveals that the B-family vortex comes from the shedding of the secondary vortex.

In Figure 7, frame (a) resembles frame (g). So frames (a) through (g) show one period of vortex shedding. The small-scale vortical structures shedding from the leading-edge are in turn captured by the primary vortex and feeding into the rolling-up process of the primary vortex. After leaving the leading-edge, both A- and B-family vortices experience severe deformation as they are stretched and captured by the primary vortex. The flow pattern inside the core of the primary vortex resembles that of the spiral instability mode, which is also observed in the experiment (Rieley & Lowson, 1998). In the numerical simulation, these small-scale vortical structures dissipate quickly as they are leaving the leading-edge and entering the central region of the primary vortex. But in the experiment the spiral instability can evolve into transition. The fast dissipation of the spiral mode in the numerical simulation can be attributed to the insufficiency of resolution. Because grids are clustered near the wall and near the leading-edge of delta wing, in the areas far away from the wall the resolution is relatively low. The future effort will be devoted to increasing the resolution where the primary vortex locates.

Because the small-scale vortical structures are shedding continuously from the leading-edge, the area near the leading-edge is of particular interesting in present work. The detailed pictures of vortex-shedding near the leading-edge is shown in Figure 8, where the limiting streamline and contours of axial vorticity of various instance on a cross-section at $x = 0.87L$ are displayed. Through (a) to (h) in Figure 8, the pattern of limiting streamline exhibits a periodic feature. Actually, figures (a) to (g) fit in one period of variation. In Figure 8(a), there is a secondary vortex attaching on the upper surface of delta wing. The strong leading-edge shear layer is shown by dark color of the contours of axial vorticity. Near the leading-edge, the shear layer is concentrated in a narrow area. In Figure 8(b), at $t = 55.68L/U_\infty$, a small vortex shown by the limiting streamline appears near the leading-edge over the free shear layer. In the same picture, a small bulge appears on the shear layer. The generation of this small vortex can be attributed to the Kelvin-Helmholtz instability. Therefore, the small vortex is named as the Kelvin-Helmholtz (K-H) type vortex. At the same time, the secondary vortex, which was attaching on the wing surface at $t = 55.54L/U_\infty$, moves away from the wall. As the K-H type vortex grows, the secondary vortex is pushed further away from the wall. From $t = 55.81L/U_\infty$ to $t = 55.95L/U_\infty$, (Figure 8(c) to (d)) the secondary vortex moves upward and begins to separate from the wall, which is corresponding to the B-family vortex, whose rotating direction is opposite to the primary vortex. Therefore, the B-family vortex comes from the shedding of the secondary vortex. The generation of the leading-edge K-H type vortex also causes the deformation of the shear layer, which is visible from the contours of the axial vorticity in Figure 8(b), (c), and (d). The bulge on the contours of axial vorticity is corresponding to the K-H type vortex. In Figure 8(d), the secondary vortex almost disappears and the K-H type vortex is still attached to the leading-edge. In Figure 8(e) and (f), the K-H type vortex grows in

size until it reaches the edge of the primary vortex. Another vortex appears at the same location of the secondary vortex, actually it is a new secondary vortex. The K-H type vortex gradually moves upward and sheds from the leading-edge, and comes out to be the A-family vortex, whose rotating direction is the same as the primary vortex. It is obviously that the A-family vortex originates from the K-H type leading-edge vortex. The last two frames are the periodic repeating of frames (a) and (b) in Figure 8.

The vortex-shedding near the leading-edge is a periodic process. The interaction between the secondary vortex and the leading-edge shear layer generates a K-H type vortex. As this K-H type vortex grows, the induced flow pushes the secondary vortex away form the wall, and ultimately leads to the shedding of the B-family vortex. The K-H type vortex grows in size as the secondary vortex shows up again near the wall. The induced flow pushes the K-H type vortex away form the wall and leads to the shedding of the A-family vortex. So the A-family vortex originates from the Kelvin-Helmholtz instability of shear flow near the leading-edge. The B-family vortex originates from the secondary vortex. The period of vortex shedding is between $0.89L/U_\infty$ and $0.98L/U_\infty$. The scale of the K-H type leading-edge vortex and the secondary vortex is about $0.005L$.

The interpretation of the above phenomena is based on the Kelvin-Helmholtz instability of cross-sectional two-dimensional flow. Considering many cross-sections simultaneously, the period of vortex shedding is the same, there is only phase difference between one cross-section and the other. From a three-dimensional point of view, the A- and B-family vortices become vortex tubes, which are oblique to the axial direction.
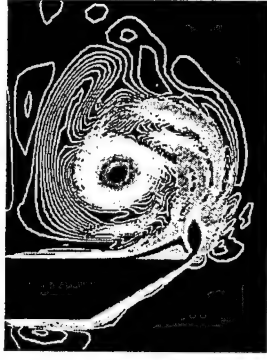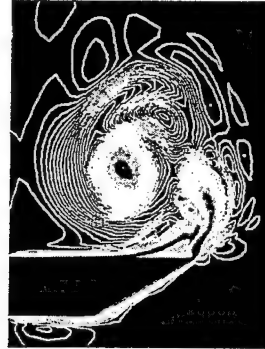
(a) $t = 55.54L/U_\infty$
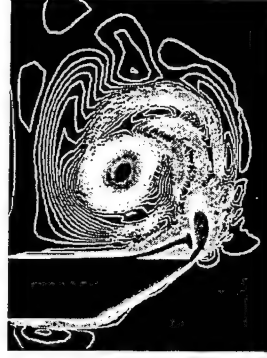
(b) $t = 55.68L/U_\infty$
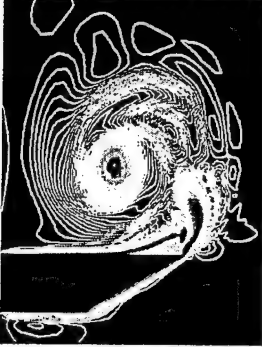
(c) $t = 55.81L/U_\infty$

(d) $t = 55.95L/U_\infty$

(e) $t = 56.09L/U_\infty$

(f) $t = 56.23L/U_\infty$

(g) $t = 56.37L/U_\infty$

(h) $t = 56.51L/U_\infty$

Figure 7: Contours of axial vorticity of different time on a cross section at $x = 0.87L$. Angle of attack $\alpha = 12.5°$, $Re = 1.96 \times 10^5$, $Ma = 0.1$

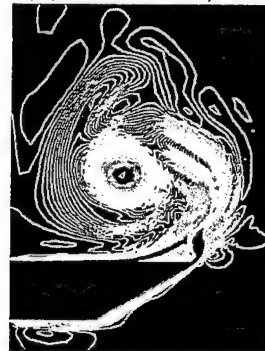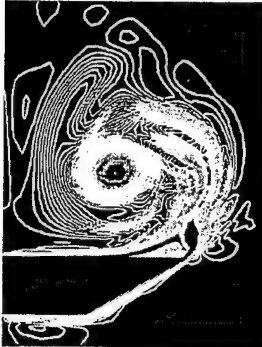(a) $t = 55.54L/U_\infty$

(b) $t = 55.68L/U_\infty$

(c) $t = 55.81L/U_\infty$

(d) $t = 55.95L/U_\infty$

(e) $t = 56.09L/U_\infty$

(f) $t = 56.23L/U_\infty$
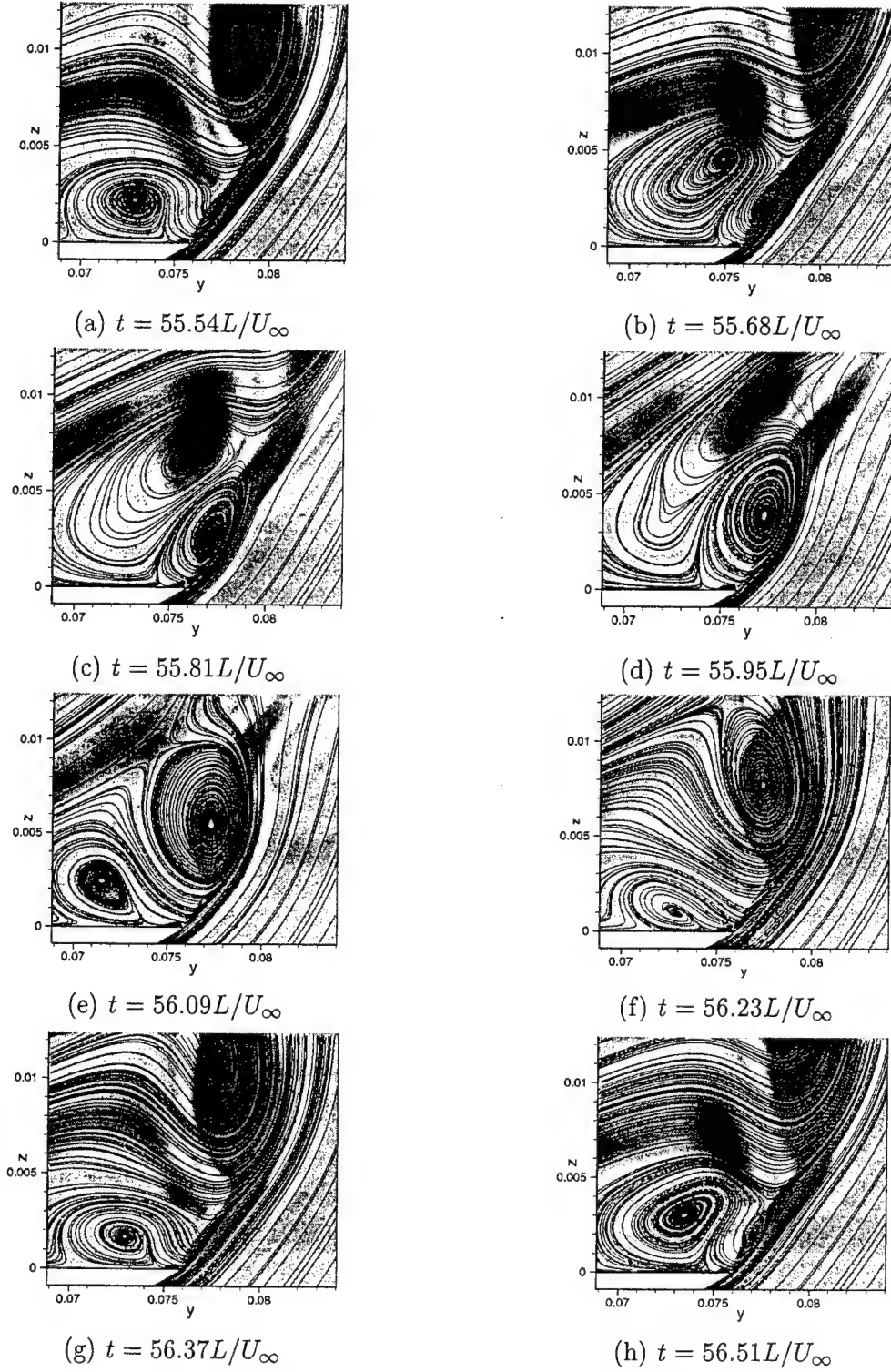
(g) $t = 56.37L/U_\infty$

(h) $t = 56.51L/U_\infty$

Figure 8: Limiting streamline and contours of axial vorticity of different time on a cross section at $x = 0.87L$. Angle of attack $\alpha = 12.5°$, $Re = 1.96 \times 10^5$, $Ma = 0.1$

3.4   History of Our DNS/LES Work

Our DNS work was initiated in 1990 by NASA Langley research grants, Multilevel Adaptive Methods for Flow in Transition, grant number NAS1-19016, NAS1-19312, NAG-1-1537. The purpose is to develop a multigrid DNS code for flow transition. The code is mainly for incompressible flow. We started to work for compressible flow transition and turbulent flow in 1994 when we received AFOSR support. Since then, we have developed efficient DNS/LES codes for both incompressible and compressible flow. We have use both DNS and LES for the whole process of flow transition on 3-D smooth and rough flat plates, 2-D airfoils and 3-D swept-wings (Liu et al, 1991a, 1991b, 1992, 1993a, 1993b, 1993c, 1994a, 1994b, 1995a, 1995b, 1996a, 1996b, 1996e, 1997a, 1997b, 1997c, 1997d; Zhao et al, 1997; Shan et al, 1999; Jiang et al, 1999a, 1999b). Some of these computational results are well validated.

We have form a strong DNS/LES team with experts in grid generation, numerical scheme, flow solver, turbulence modeling, and visualization, which consists of 1 faculty, two post doctors, and two PhD students. The AFOSR grant supports faculty and post doctors while Louisiana Tech supports two PhD students.

The features of DNS research by the Louisiana Tech Team include the following:

- The whole process of flow transition including receptivity, linear growth, non-linear instability, breakdown, and transition to turbulence.

- Detailed simulation of flow separation, wakes, interaction between separation and wakes, noise generation by T-S wave and wakes.

- General geometry including 2-D and 3-D airfoils with different attack angles.

- Medium Reynolds number up to 10^6.

- All speeds, including incompressible, subsonic, and supersonic flows.

4   Other Supporting Information

4.1   Institutional Description

Louisiana Tech University is a comprehensive public university committed to quality in teaching, research, creative activity, and public service. Today, Louisiana Tech has over 10,000 students. Integral to the purpose of the University is its expanding commitment to graduate education. Recent additions of two PhD programs and efforts to form internationally competitive research centers are strong evidence of this expanding commitment to world class research and graduate education.

As a university with a rich engineering heritage, Louisiana Tech has a special responsibility to integrate advanced technology into teaching and learning. At Tech, advanced technology supports quality teaching, research, and service. The university is committed to providing its students with

advanced technological skills that help to ensure their success in the University and in the wider surrounding community.

The College of Engineering and Science (COES) at Louisiana Tech consists of Biomedical Engineering, Chemical Engineering, Chemistry, Civil Engineering and Geoscience, Computer Science, Electrical Engineering, Mechanical Engineering, Mathematics and Statistics, Physics, and Industrial Engineering. All programs offer the Master degree. COES has also four doctoral programs, including Ph.D. in Applied Computational Analysis and Modeling (ACAM), Ph.D. in Biomedical Engineering, Ph.D. in Engineering, and Doctor of Engineering. The ACAM curriculum is an interdisciplinary doctoral degree program administered by the Graduate School, with participation from the College of Engineering and Science (including Computer Science, Mathematics and Statistics). The program is intended to produce professionals with a firm grasp of the fundamentals of mathematical modeling who also have the expertise to implement, analyze and evaluate such models using state-of-the-art computing environments and advanced visual data analysis techniques. The project team includes a number of ACAM faculty and students.

The Center for Numerical Simulation and Modeling is a nationally and internationally recognized research group for its efforts in use of direct numerical simulation (DNS) and large eddy simulation (LES) techniques with multigrid refinement in analysis of three-dimensional turbulent and transitional flows. They are one of the major research centers in the nation to conduct DNS/LES for complex geometries.

4.2   Maintenance of Existing Equipment

We purchased the SGI Origin 2000 wth 16 CPUs and 4 GB memory by an AFOSR grant and Louisiana Tech matching fund. We have a three-year free maintenance contract with SGI who provides all software and on-site hardware support free for three years, 1998-2001. CNSM is in charge to manage the system and the University provides a 1/4 technician to help maintain the system. After using it for one year, we found the system is well maintained and managed. We only had a very few interruptions because of the defect of some parts and SGI fixed it very quickly. It is clearly shown we have ability to maintain the upgraded system and the new ImmersaDesk. La Tech has got a new three-year free maintenance contract with SGI for the new upgraded system.

4.3   Estimated Life of the Equipment

Usually, a new advanced computer could be thought of as an advanced machine for at least three years, and will be considered useful for another 5 years. Therefore, the SGI Origin 2000 can be used for the next 5 years. The ImmersaDeskis estimated to be used for the next 5-8 years before the industry develops new advanced and inexpensive virtual reality system.

References

[1] Agrawal, S., Barnett, R. M., and Robinson, B. A. 1992. Numerical investigation of vortex breakdown on a delta wing. *AIAA Journal*, **30**(3), pp.584–591.

[2] Cipolla, K. M., Liakopoulos, A., and Rockwell, D. O. 1998. Quantitative imaging in proper orthogonal decomposition of flow past a delta wing. *AIAA Journal*, **36**(7), pp.1247–1255.

[3] Cipolla, K. M., and Rockwell, D. 1998. Small-scale vortical structures in crossflow plane of a rolling delta wing. *AIAA Journal*, **36**(12), pp.2276–2278.

[4] Gad-el-Hak, M., and Balckwelder, R. F. 1985. The discrete vortices from a delta wing. *AIAA Journal*, **23**(6), pp.961–962.

[5] Gordnier, R. E., and Visbal, M. R. 1994. Unsteady vortex structure over delta wing. *Journal of Aircraft*, **31**(1), pp.243–248.

[6] Jiang, L., Shan, H., Liu, C., Direct numerical simulation of boundary-layer receptivity for subsonic flow around airfoils, the 2nd AFOSR International Conference on DNS/LES, June, 1999a.

[7] Jiang, L., Shan, H., Liu, C., Non-reflecting boundary conditions in curvilinear coordinates, the 2nd AFOSR International Conference on DNS/LES, June, 1999b.

[8] Lele, S. K., Compact finite difference schemes with spectral-like resolution. *J. Comput. Phys.*, **103**, pp.16–42, 1992.

[9] Liu, C., Liu, Z., and McCormick, S., Multilevel adaptive methods for incompressible flow in grooved channels, *J. Comput. Appl. Math.* **38**, 283-295, 1991b.

[10] Liu, Z. and Liu, C., Fourth order finite difference and multigrid methods for modeling instabilities in flat plate boundary layers. *J. of Wind Engineering* **52**, 412–417, 1992.

[11] Liu, C. and Liu, Z., High order finite difference and multigrid methods for spatially-evolving instability. *J. Comput. Phys.*, **106**, 92-100, 1993a.

[12] Liu, C., and Liu, Z., Multigrid Methods and High Order Finite Difference for Flow in Transition – Effects of Isolated and Distributed Roughness Elements, *AIAA 93-3354*, 1993b.

[13] Liu, C., Liu, Z., and McCormick, S., Multigrid methods for flow transition in three-dimensional boundary layers with surface roughness, *NASA Contractor Report 4540*, September, 1993c.

[14] Liu, Z. and Liu, C., Fourth order finite difference and multigrid methods for modeling instability in flat plate boundary layers - 2-D and 3-D approaches, *J. Computers and Fluids*, Vol 23, No.7, pp. 995-982, 1994a.

[15] Liu, Z., Liu, Z. X., Liu, C., and McCormick, S., Multilevel methods for temporal and spatial flow transition simulation in a rough channel, *International Journal for Numerical Methods in Fluids*, Vol 18, 1994b.

[16] Liu, C., and Liu, Z., Multiple scale simulation for transitional and turbulent flow, *AIAA 95-0777*, 1995a.

[17] Liu, C., and Liu, Z., Multigrid mapping and box relaxation for simulation of the whole process of flow transition in 3-D boundary layers, *J. Comput. Phys.*, **119**, pp.325-341, 1995b.

[18] Liu, Z., Xiong, G., and Liu, C, Direct numerical simulation for the whole process of transition on 3-D airfoils, *AIAA 96-2081*, 1996a.

[19] Liu, Z., Xiong, G., and Liu, C., Leading edge receptivity to the freestream vortical disturbance of 2-D and 3-D airfoils, *AIAA 96-2084*, 1996b.

[20] Liu, C. and Guo, Y., High-order grid generation and its application in DNS, *Proceeding of 5th International Conference on Numerical Grid Generation in Computational Fluid Dynamics and Related Fields*, Mississippi State University, April 1–5, 1996c.

[21] Liu, C., Principles in multilevel adaptive methods , Lecture notes, *ACFD Short Course* (Liu, C. and Liu, Z. eds), pp. 239 - 264, Louisiana Tech University, June 24-28, 1996d.

[22] Liu, C., DNS for flow transition around complex geometry , Lecture notes, *ACFD Short Course*, Louisiana Tech University, pp. 343 - 376, Edited by Liu, C. and Liu, Z., June 24-28, 1996e.

[23] Liu, Z., Zhao, W., and Liu, C., Direct numerical simulation of transition in a subsonic airfoil boundary layer, *AIAA Paper 97-0752*, 1997a.

[24] Liu, Z., Zhao, W., and Liu, C., Direct numerical simulation of transition in high-speed boundary layers around airfoil, *AIAA Paper 97-0753*, 1997b .

[25] Liu, C. and Liu, Z., Direct Numerical Simulation for Flow Transition Around Airfoils, *Proceedings of First AFOSR International Conference on DNS/LES, Louisiana Tech University, Ruston, Louisiana*, August 4-8, 1997c, pp13-28, Edited by C. Liu, Z. Liu and L. Sakell.

[26] Liu, Z., Zhao, W., and Liu, C., Direct Numerical Simulation of Flow Transition in a Compressible Swept-Wing Boundary Layer, *Proceedings of First AFOSR International Conference on DNS/LES, Louisiana Tech University, Ruston, Louisiana*, August 4-8, 1997d, pp223-232, Edited by C. Liu, Z. Liu and L. Sakell.

[27] Liu, C., Zheng, X., and Sung, C., Preconditioned multigrid methods for unsteady incompressible flows, J. of Computational Physics, No. 139, pp. 35-37, 1998.

[28] Modiano, D. L., and Murman, E. M. 1994. Adative computations of flow around a delta wing with vortex breakdown. *AIAA Journal*, **32**(7), pp.1545–1547.

[29] Poinsot, T. J., Lele, S. K., Boundary conditions for direct simulations of compressible viscous flows, *J. Comput. Phys.*, **101**, pp 104–129, 1992.

[30] Riley, A. J., and Lowson, M. V. 1998. Development of a three-dimensional free shear layer. *J. Fluid Mech.*, **369**, pp.49–89.

[31] Payne, F. M., Ng, T. T., Nelson, R. C., and Shiff, L. B. 1988. Visualization and wake surveys of vortical flow over a delta wing. *AIAA Journal*, **26**(2), pp.137–143.

[32] Shan, H., Jiang, L., Zhao, W., Liu, C., "Large eddy simulation of flow transition in a supersonic flat-plate boundary layer". AIAA Paper 99-0425, the 37th AIAA Aerospace Sciences Meeting and Exhibit, Reno, NV, Jan. 11-14, 1999.

[33] Spekreijse, S.P. (1995) Elliptic grid generation based on Laplace equations and algebraic transformation. *J. Comp. Phys.*, **118**, pp.38–61

[34] Visser, K. D., and Nelson, R. C. 1993. Measurements of circulation and vorticity in the leading-edge vortex of a delta wing. *AIAA Journal*, **31**(1), pp.104–111.

[35] Yoon, S., Kwak D. Implicit Navier-Stokes solver for three-dimensional compressible flows, *AIAA Journal* **30**, pp.2653-2659, 1992.

[36] Zhao, W., Liu, Z., and Liu, C., Numerical Investigation of Flow Transition in a Supersonic Airfoil Boundary Layer, *Proceedings of First AFOSR International Conference on DNS/LES, Louisiana Tech University, Ruston, Louisiana*, August 4-8, 1997, pp257-264, Edited by C. Liu, Z. Liu and L. Sakell.

22